

Palaeomagnetic study of the Xitle-Pedregal de San Angel lava flow, southern Basin of Mexico

J. Urrutia-Fucugauchi

Laboratorio de Paleomagnetismo y Geofísica Nuclear, Instituto de Geofísica, Universidad Nacional Autónoma de México, D. Coyoacán 04510 D.F., México

Received 15 February 1994; revised 17 November 1995; accepted 1 December 1995

Abstract

A detailed study of the ~2000 years old Xitle-Pedregal de San Angel volcanic field in the southern Basin of Mexico was undertaken to assess the reliability of the palaeomagnetic record as derived from fresh well-preserved and exposed lava flows. The Xitle vent is on the slope of the Ajusco volcano, which results in a topographic difference of over 800 m in less than 12 km of horizontal distance. Most sites present a mean direction, with a small within-site dispersion, around the dipolar direction for the locality, but some sites, particularly in the basin sector of flat relief away from the vent, show shallow inclinations. Anisotropy of magnetic susceptibility (AMS) shows normal 'flow' fabrics with horizontal foliation planes and small anisotropy degree. AMS lineations correlate with observed flow directions. The magnetic properties vary systematically across flow units, but directions do not show a consistent pattern. Secular variation effects do not apparently contribute to the shallow inclinations or directional scatter. Some lava structures like pressure crests and blocky fronts give shallow inclinations and scattered directions, respectively. The resulting overall mean direction is well defined and close to the dipolar direction ($B = 26$, Dec = 359.8°, Inc = 32.8°, $k = 167$, $\alpha_{95} = 2.2^\circ$), but this excludes two apparent directional groups. The mean direction for one group, with $B = 19$, Dec = 359.0°, Inc = 35.1°, $k = 247$, $\alpha_{95} = 2.1^\circ$, may be the representative estimate for the field. Shallow inclinations are considered anomalous and associated to a characteristic specific to given sectors of lava flows. Palaeointensity determinations have been obtained for six samples from five sites by using the Thellier and Shaw methods. Results agree well with previous studies, however, the standard deviation calculated for the mean value remains high after incorporation of the new data. Mean palaeointensity based on five new determinations and eight early data is $N = 13$, 56.50 ± 6.16 mT (and the mean for the overall data set is $N = 20$, 60.50 ± 9.21 mT). Results illustrate some practical considerations and limitations in methodology and the reliability of the palaeomagnetic record in volcanic rocks.

1. Introduction

The Xitle-Pedregal de San Angel volcanic field is formed by fresh, well exposed basaltic lava flows that originated from the activity of the Xitle cinder cone some 2000 years ago in the southern sector of the Basin of Mexico (Fig. 1). Earlier palaeomagnetic

studies in the 1970s (Mooser et al., 1974; Urrutia-Fucugauchi and Valencio, 1976; Herrero-Bervera and Pal, 1978) reported data for the lava flows with small within-site dispersions but with different mean directions. In particular, there were nine sites with inclinations close to the dipolar value and five sites with inclinations some 10°–12° shallower (Table 1). Only

one site showed a steep inclination (Herrero-Bervera and Pal, 1978). The dipolar inclination for the area varies between 34.93° to 35.06°. The ‘shallow inclination’ group had a mean direction of Dec = 3.4°, Inc = 25.6° ($\alpha_{95} = 2.1^\circ$, $k = 558$, $B = 5$) and the

‘close to dipolar’ group has a mean direction of Dec = 358.6°, Inc = 35.0° ($\alpha_{95} = 2.9^\circ$, $k = 316$, $B = 9$) (Table 1). The two groups are statistically different (McFadden and Lowes, 1981) and have cones of 95% confidence that do not overlap. Since

Table 1
Summary of paleomagnetic data for the Pedregal de San Angel, southern Basin of Mexico

Site	<i>N</i>	Dec	Inc	<i>k</i>	α_{95}	ΔI	Ref.
<i>Previous data</i>							
MNN-14	7	6.7	24.7	104	6.0	−10.3	1
MNN-15	8	354.9	38.8	429	2.7	3.3	1
HP-6	17	358.0	34.3	301	2.1	−0.7	2
HP-7	11	354.6	33.7	86	5.0	−1.3	2
HP-8	9	7.2	33.4	51	7.3	−1.6	2
HP-9	8	4.5	27.1	115	5.2	−7.9	2
HP-10	9	6.0	34.9	118	4.8	−0.1	2
HP-13	8	355.1	38.9	114	5.2	3.9	2
HP-14	8	356.8	52.3	151	4.5	17.3	2
HP-15	7	356.1	33.6	62	7.7	1.4	2
JU-1	6	5.0	23.7	72	7.9	−11.3	3
JU-2	8	3.0	25.7	62	7.1	−9.3	3
JU-3	8	357.6	26.7	73	6.5	−8.3	3
JU-4	17	358.4	34.3	301	2.1	−0.7	3
UM-1	6	356.5	32.3	276	4.0	−2.7	4
Mean (shallow inclination sites)	<i>B</i> = 5	3.4	25.6	558	2.1	−9.4	
Mean (close-to-dipolar sites)	<i>B</i> = 9	358.6	35.0	316	2.9	0.0	
Overall mean (without HP-14)	<i>B</i> = 14	0.4	31.7	155	3.2	−3.3	
Overall mean (all sites)	<i>B</i> = 15	0.2	33.0	97	3.9	−3.0	
<i>Recent data</i>							
CU-1	6	357.0	34.9	477	3.1	−0.1	
CU-2	6	353.6	36.2	151	4.5	1.2	
CU-3	5	5.3	41.1	217	4.6	6.1	
CU-5	5	347.9	15.2	293	4.5	−19.8	
CU-8	15	357.0	36.7	61	5.1	1.7	
XT-4	6	359.7	34.6	295	3.9	−0.4	
XT-6	9	355.3	37.0	123	4.7	2.0	
XT-7	6	1.1	32.9	265	4.1	−2.1	
XT-9	7	350.1	31.8	395	3.0	−3.2	
CC-1	7	4.4	32.2	119	5.5	−2.8	
IN-4	4	357.6	28.4	41	8.7	−6.6	
P-8	8	355.9	29.9	67	6.8	−5.1	
XP-6	5	11.4	33.4	66	9.5	−1.6	
Mean (without CU-5 and XP-6)	<i>B</i> = 11	357.9	34.2	247	2.9	−1.8	
Mean (without CU-5)	<i>B</i> = 12	359.0	34.2	189	3.2	−1.8	
Overall mean (shallow inclination sites)	<i>B</i> = 7	1.5	26.7	338	3.3	−8.3	
Overall mean (close-to-dipolar sites)	<i>B</i> = 19	359.0	35.1	247	2.1	0.1	
Overall mean	<i>B</i> = 28	359.2	32.9	100	2.7	−2.1	
Overall mean (without CU-5 and HP-14)	<i>B</i> = 26	359.8	32.8	167	2.2	−2.2	

N, number of samples; Dec/Inc, mean declination and inclination; *k*, α_{95} , Fisher statistical parameters; ΔI , inclination anomaly; Ref., reference. 1, Mooser et al. (1974); 2, Herrero-Bervera and Pal (1978); 3, Urrutia-Fucugauchi and Valencio (1976); and 4, Urrutia-Fucugauchi and Martin del Pozzo (1993).

there were apparently no indications for secondary components or tectonic effects, the occurrence of the two groups was difficult to explain.

The overall mean direction for the Xitle-Pedregal de San Angel field has been obtained by averaging all sites and it could be considered well defined, with $\alpha_{95} = 3.9^\circ$ and $k = 97$ (Table 1). However, this ignores the occurrence of the two groups. Furthermore, the shallow inclination sites came mainly from a particular area in the university campus (Fig. 1). The present study grew from an attempt to document this apparent anomaly and was then extended to investigate the reliability of the palaeomagnetic record in young fresh volcanic rocks as studied using current methods.

2. Xitle-Pedregal de San Angel field and sampling

The Xitle-Pedregal de San Angel volcanic field extends over a wide area in the southern sector of the Basin of Mexico. Lava flows cover some of the earlier pyramids and settlements in the region (Cuicuilco and Copilco archaeological sites). Nowadays, Mexico City has extended over the lava field and the National University, including the Paleomagnetism Laboratory, is built on top of the flows.

Organic material associated with the eruption of Xitle volcano was dated early during development of the radiocarbon method (Arnold and Libby, 1951; Libby, 1955). This date of 2422 ± 250 years BP (before present, AD 1950) (C-200; Table 2) remains as the most widely quoted age for the Xitle eruption in subsequent studies; although there have been several additional studies reported (available data is summarized in Table 2), the age has remained a matter of controversy (Heizer and Bennyhoff, 1958, 1972; Ortega et al., 1993). Some studies have supported a much younger age for the Xitle; for instance, Cordova et al. (1994) have recently selected the date reported by Fergusson and Libby (1963) of 1536 ± 65 years BP (UCLA-228) which had been correlated with archaeological remains covered by the lava. Dates show three apparent groups, roughly around 2000, 2375, and 4000 years BP (Fig. 2). The group around 4000 years BP is mainly formed by dates obtained in the Cuicuilco archaeological excavations from horizons between about 4 and 7 m below the ground level and lava contact. They can be related to early archaeological occupation Tlalpan stages (Fergusson and Libby, 1963). The second group includes the date by Arnold and Libby (1951) which was obtained from a soil collected underneath the lava in Cuicuilco. The date of 2000 years BP for the first group has also been proposed as the age for the Xitle eruption (e.g. Heizer and Bennyhoff, 1958; White et al., 1990). We favour this date as representative for the eruption, mainly because of the relative position of the material dated with respect to the lava and ash. A radiocarbon age determination on a burned wood fragment we collected beneath the lava (Ortega et al., 1993) in a quarry to the southeast of the Universidad Nacional Autonoma de Mexico (UNAM) campus gives a (C-13 corrected) date of 1960 ± 65 years BP (Geochron Laboratory, Krueger Enterprises

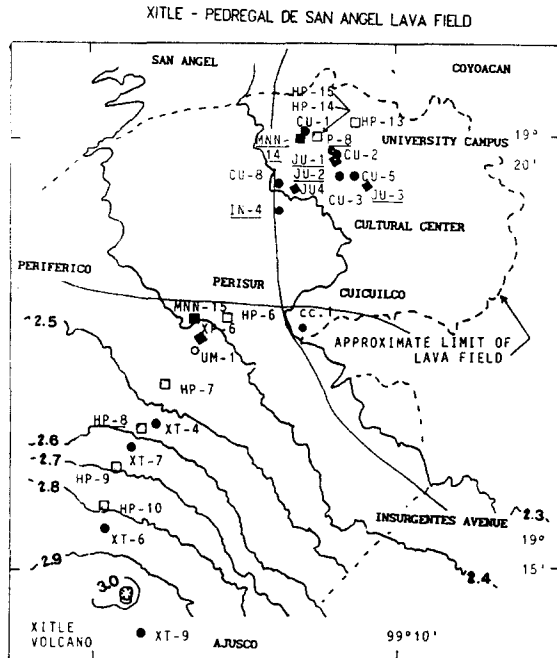


Fig. 1. Schematic map of the Xitle-Pedregal de San Angel volcanic field (adapted from Badilla-Cruz, 1977 and Schmitter, 1953) showing location of new sampling sites (indicated by the closed circles). For a list of sites refer to Table 1. Approximate location of sites from previous studies are indicated by the other symbols. Topographic contours every 100 m and some major streets and the university campus are added for reference. The Xitle cinder cone grew on the slope of the large Ajusco volcano complex and the lava flows were emplaced to the north-northeast following the topographic relief (see also Fig. 15). The sites showing shallow mean inclinations are underlined (see Table 1 and text).

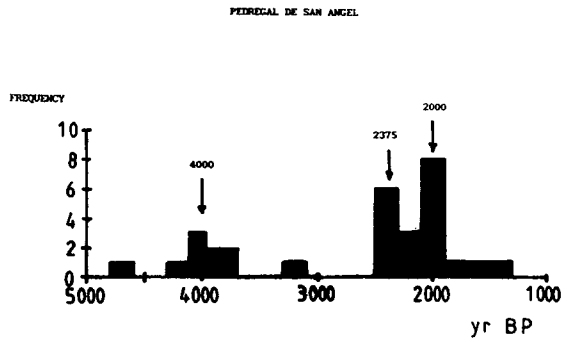


Fig. 2. Histogram of radiocarbon dates that are related to volcanic units in the southern Basin of Mexico. Note the apparent occurrence of three major groups, around 2000, 2375, and 4000 years BP (see text for discussion).

Inc., USA). This date agrees with the date reported by White et al. (1990) for a wood fragment from a nearby site (1960 ± 70 years BP; TX-3648) and two dates reported by Cordova et al. (1994) (TX-7668 and TX-7669). Correction of the conventional radiocarbon date of 1960 years BP with reference to the dendrochronological curve (Fig. 3) gives a date of 1890 years BP (AD 60). All conventional radiocarbon dates have been corrected by reference to the dendrochronological time scales reviewed recently by Stuiver and Becker (1993) and Stuiver and Pearson (1993), and are graphically illustrated in Fig. 3 (also referred to calendar years). Conventional radiocarbon dates agree with the dendrochronological

Table 2
Radiocarbon dates of Xitle-Pedregal de San Angel lava field

Sample	C^{14} ($\pm \sigma$) years BP	Cal C^{14}	Calendar	Reference
M-664	1430 ± 200	1309	AD 642	CG-58
UCLA-228	1536 ± 65	1409	AD 541	FL-63
UCLA-205	1790 ± 75	1645	AD 305	FL-63
Y-437	1925 ± 60	1870 (1855)	AD 70 (AD 95)	DGH-59
UCLA-206	1950 ± 80	1885	AD 55	FL-63
TX-3648	1960 ± 70	1890	AD 60	WROV-90
G-1000	1960 ± 65	1890	AD 60	OUN-93
TX-7669	2030 ± 60	1970	20 BC	CML-94
M-663	2040 ± 200	1975	25 BC	CG-58
TX-7668	2090 ± 70	2040	90 BC	CML-94
UCLA-208	2100 ± 75	2050	100 BC	FL-63
UCLA-602	2190 ± 80	2150 (2295)	200 BC (335 BC)	FL-63
UCLA-603	2230 ± 80	2205 (2310)	245 BC (340 BC)	FL-63
UCLA-209	2300 ± 70	2335	385 BC	FL-63
C-200	2422 ± 250	2420	465 BC	AL-52
M-662	2450 ± 250	2450	500 BC	CG-58
UCLA-595	2490 ± 100	2510	560 BC	FL-64
UCLA-594	2560 ± 100	2720	770 BC	FL-64
UCLA-596	2560 ± 80	2720	770 BC	FL-64
UCLA-207	2600 ± 70	2740	790 BC	FL-63
UCLA-597	3320 ± 100	3350	1580 BC	FL-64
UCLA-599	3850 ± 200	4230	2280 BC	FL-63
UCLA-598	3820 ± 100	4225	2275 BC	FL-63
UCLA-600	3930 ± 100	4400	2450 BC	FL-63
UCLA-210	3980 ± 60	4420	2470 BC	FL-63
UCLA-212	4050 ± 75	4520	2570 BC	FL-63
UCLA-601	4110 ± 120	4605	2655 BC	FL-63
TX-7670	4690 ± 70	5450	3500 BC	CML-94

Laboratory codes are: UCLA, University of California at Los Angeles; M, University of Michigan; Y, Yale University; C, University of Chicago; TX, University of Texas at Austin; G, Geochron Laboratories, Inc. References are: AL-52, Arnold and Libby (1951); CG-58, Crane and Griffin (1958); CML-94, Cordova et al. (1994); DGH-59, Deevey et al. (1959); FL-63, Fergusson and Libby (1963); FL-64, Fergusson and Libby (1964); OUN-93, Ortega et al. (1993); WROV-90, White et al. (1990). The calibrated dates have been referred to the dendrochronology calibration curves of Stuiver and Becker (1993) and Stuiver and Pearson (1993). Calendar dates are referred to the standard Julian time scale.

centimetres thick can also be found in some sites in the basin (e.g. in the archaeological sites). There is no soil or ash between the flow units.

Previous studies have concentrated on the low areas in and around the university campus. Therefore sampling was extended into the Ajusco slope towards the Xitle vent (Fig. 1). Examination of these results then prompted additional sampling campaigns in the lower areas in order to evaluate some possible factors affecting the palaeomagnetic record and also to investigate particular structures (e.g. pressure crests and lava blocky fronts). A total of 14 new sites, with some five to 15 samples per site, were collected.

3. Methods and results

Previous studies used magnetic compass orientation, therefore for this study both solar and magnetic compass orientations were used in order to evaluate the influence of the outcrop magnetizations on the orientation procedures. There were angular differences of about $\pm 5^\circ$ and up to 16° between the two

orientation schemes. Angular differences do not seem to follow a simple trend as a function of initial magnetization intensity (Fig. 4). Magnetization directions used for the site mean calculations (and statistics) below have been corrected using the solar compass orientations. However, site mean directions calculated using the solar and magnetic compass orientations are not significantly different, only within-site angular dispersion is less for the solar compass.

The intensity and direction of natural remanent magnetization (NRM) were measured with a Mol-spin spinner magnetometer attached to an IBM computer. Low-field susceptibility was measured with the Minisep instrument. Vectorial composition, coercivity and unblocking temperature spectra were investigated by detailed step wise alternating field (AF) and thermal demagnetization. AF demagnetization was completed in 8–12 steps up to 100 mT in a reverse tumbling Schonstedt demagnetizer. Thermal demagnetization was done in 8–10 steps up to 580°C in a Schonstedt TSD-1 demagnetizer.

Characteristic magnetization directions were estimated from end-point analysis and the vector plots. Characteristic magnetizations were obtained from last

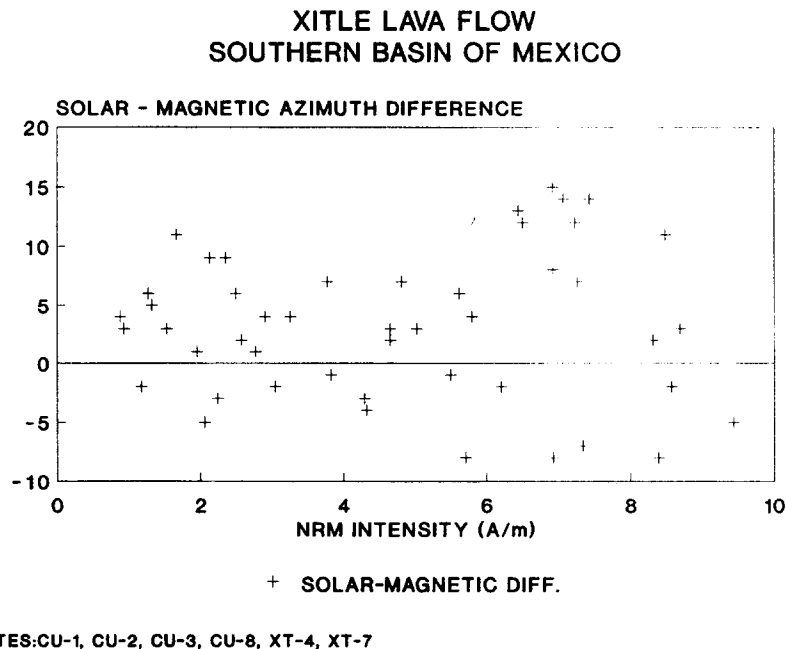


Fig. 4. Angular difference between the solar and the magnetic compass orientation plotted as a function of NRM intensity for individual samples.

vector segments going through the origin (some good and regular examples are illustrated in Fig. 5). Site-mean directions were calculated by vector addition giving unit weight to sample directions. Fisher statistics were used to estimate dispersion parameters (Fisher, 1953; Irving, 1964). Results are summarized in Table 1. The within-site angular dispersion was low, with k varying from 41 to 447. The overall mean direction ($B = 12$, without site CU-5) is well grouped, with a k of 189 and α_{95} of 3.2° (Table 1). However, it is not a great improvement over the previous estimate. Elimination of site XP-6 that presents the highest within-site dispersion ($k = 66$, $\alpha_{95} = 9.5^\circ$) improves the grouping ($k = 247$, $\alpha_{95} = 2.9^\circ$, $B = 11$) (Table 1), but there are no compelling reasons to eliminate this site from the final calculations.

Isothermal remanent magnetization (IRM) acquisition experiments were done with a home-made

pulse magnetizer. IRM curves vary with the relative position of the sample within the flow. Samples from the top portions show saturation at about 400 mT, where as samples from the bottom show a slight increase up to 800 mT (e.g. Fig. 6). Comparison of AF coercivity spectra for NRM and saturation IRM (Fig. 6(b)) suggest the occurrence of single or pseudo-single domain magnetic minerals (Lowrie and Fuller, 1971). Further analysis of coercivity spectra with estimation of the coercivity (H_c), remanent magnetization/saturation remanence ratio (M_r/M_s), and coercivity/coercivity of remanence ratio (H_{cr}/H_c) was completed with the MicroMag system. An example of the hysteresis loop and saturation remanence is given in Fig. 7. Curie temperature estimates were derived from thermomagnetic curves obtained in a horizontal Curie balance with inducing fields of around 0.8 T. Just three samples were

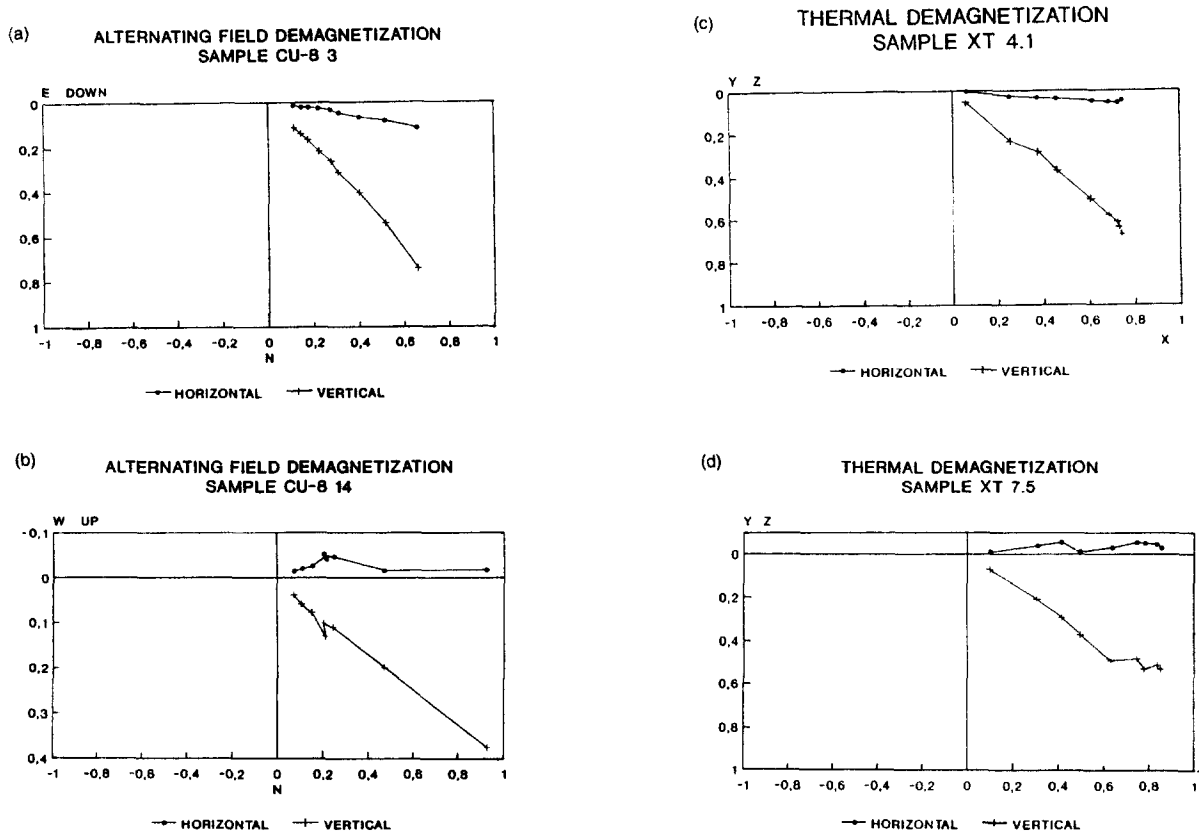


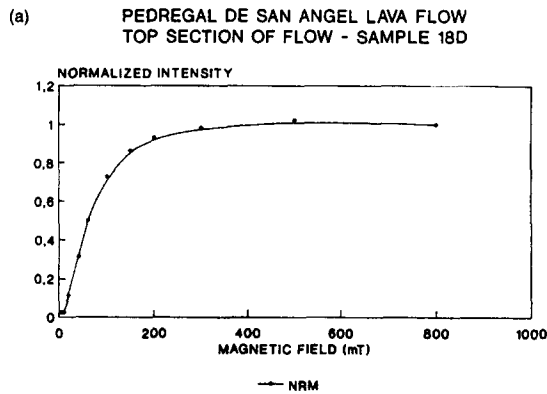
Fig. 5. Examples of vector plots for samples of the Xitle-Pedregal de San Angel lavas, after AF ((a) and (b)) and thermal ((c) and (d)) demagnetization.

analysed and the Curie temperature estimated is around 575°C, corresponding to pure magnetite (Fig. 8). The thermomagnetic curves show irreversible behaviour, indicating alteration of the sample during the heating cycle. We also noted that in some samples, unblocking temperatures were as low as 300°C, suggesting magnetite of a particular grain size or maghemite. No thermomagnetic curves were obtained for those samples, but Nagata et al. (1965) reported three examples with two Curie points of 300°C plus 520°, 530°, and 570°C, respectively, for a locality close to the archaeological site of Cuicuilco. In addition, they reported Curie point estimates for seven samples that ranged from 500° to 570°C (and two cases with lower Curie temperatures that they labelled with a question mark without further com-

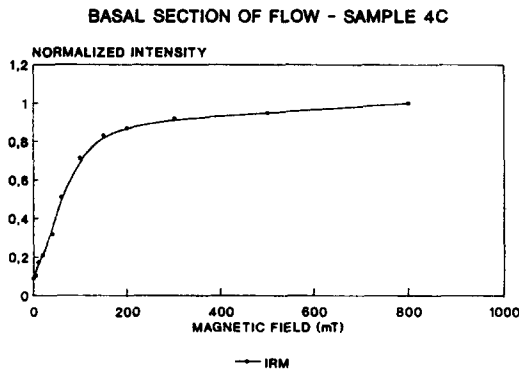
ment). Two examples illustrated in Nagata et al. (1965) display a nearly reversible behaviour during the heating cycle (also conducted in air).

Ore petrology observations using the oil immersion technique on polished sections were carried out on samples from one site CU-8. Abundant euhedral titanomagnetite grains from 20 to 100 μm and up to 150–160, with high deuteric oxidation stages characterize the samples. Titanomagnetite grains show ilmenite and hematite intergrowths with characteristic Trellis textures. Oxidation corresponds to classes of C-4 and C-5 for titanomagnetite and R-5 of Haggerty (1976).

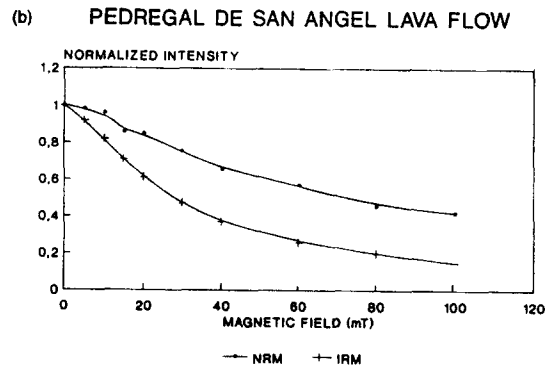
In some of the sites, samples were collected from the different flow units and also spaced from base to top of the flow (e.g. Fig. 9). Magnetic properties



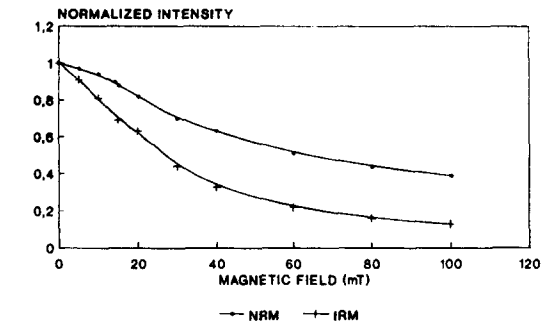
SATURATION IRM 46.28 A/m



SATURATION IRM 76.8 A/m



TOP SECTION OF FLOW - SAMPLE 18D



BASE OF FLOW - SAMPLE 4C

Fig. 6. Examples of isothermal remanent magnetization (IRM) acquisition curves for samples from the upper (above) and lower (below) portion of a lava flow. Comparison of the coercivity spectra for natural remanent magnetization (NRM) and isothermal remanent magnetization (IRM). Examples for a (above) sample from upper part of a lava flow and a (below) sample from lower part of a lava flow.

vary across the flow, with susceptibility and NRM intensity increasing in the basal section and particularly towards the top (Fig. 9(a)). The coercivity and unblocking temperature spectra show an apparent pattern, indicating a relationship with grain size (and/or oxidation states). However, there is no noticeable pattern in the variation of the directions (Fig. 9(b)), and clearly no indication of ‘shallow inclination’ sectors. Results are similar to those reported

earlier for several vertical sections by Centeno-Garcia et al. (1986), which were interpreted in terms of oxidation degree within the flow units.

Anisotropy of magnetic susceptibility (AMS) was measured with the Minisep instrument. AMS principal directions show ‘normal flow’ fabrics with foliation planes almost horizontal and lineation around the flow direction observed from field indicators (Fig. 10(a)). The anisotropy degree is small, less

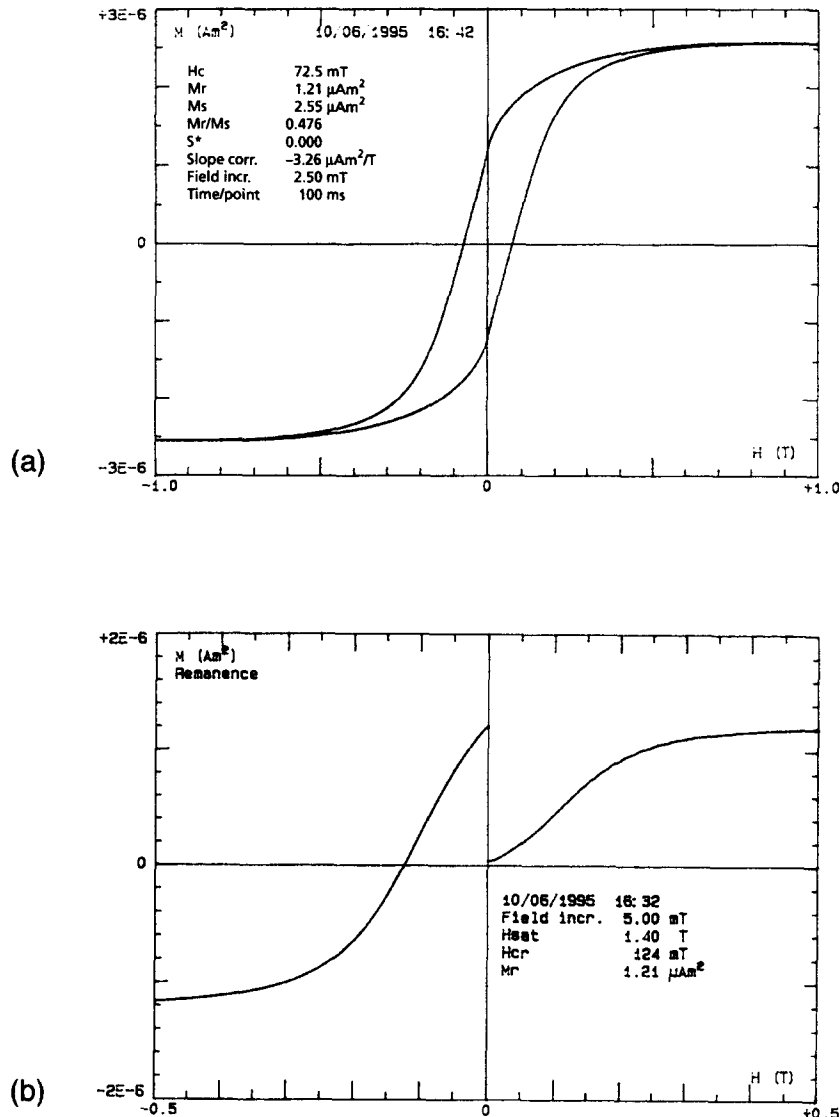


Fig. 7. Example of a hysteresis loop (a) and IRM curve and back field curve (b) obtained with the MicroMag system. Example from site CU-8.

than 2% (Fig. 10(b)) and samples seem predominantly foliated (Fig. 10(c)). There seems to be no relationship with NRM directions, so there is no apparent effect of AMS on remanence directions.

Palaeointensity determinations were completed by using the Thellier method (Thellier and Thellier, 1959) (as modified by Coe and Grommé, 1973) and by the Shaw single heating method (Shaw, 1974). Samples selected for the palaeointensity study were

those that for the particular site (in a previously demagnetized companion specimen) showed small or preferably negligible low-coercivity or low-unblocking temperature (viscous) components. We obtained four reliable determinations using the Thellier method and two using the Shaw method. Examples of the experimental data using the Thellier and the Shaw methods are given in Fig. 11 and Fig. 12. Results are summarized in Table 3. Also tabulated

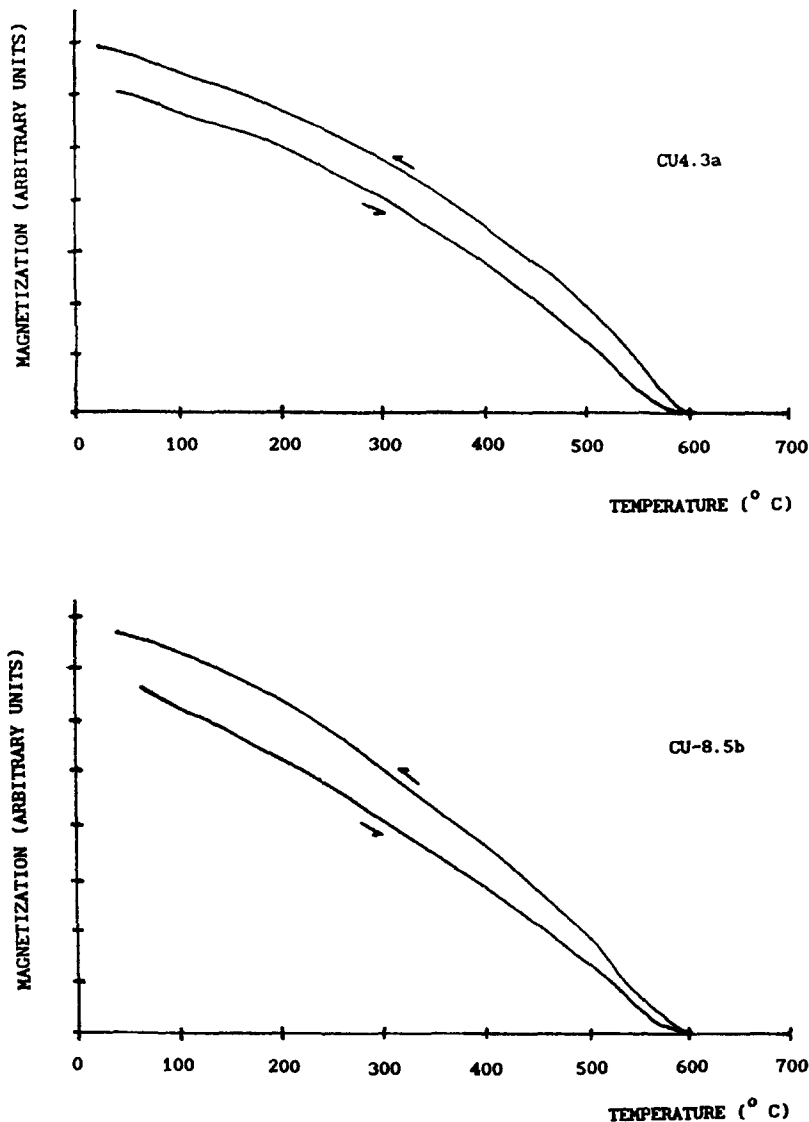


Fig. 8. Example of two thermomagnetic curves for samples of sites CU-4 and CU-8, showing a Curie point of about 575°C corresponding to pure magnetite.

are the results reported by Nagata et al. (1965) and Gonzalez-Huesca (1992). The mean value for the six determinations is 60.04 ± 9.62 mT, which is higher than the mean value calculated for the results reported by Nagata et al. (1965) and lower than that for the results of Gonzalez-Huesca (1992). The data reported in Gonzalez-Huesca (1992) appear consistently higher than those in Nagata et al. (1965) and this study. If sample XT-4.1 is not included in the average, the mean is $N = 5$, 57.13 ± 7.23 mT, quite close to the mean of 56.11 ± 5.89 mT calculated for the Nagata et al. (1965) samples (Table 3). The mean for the two sets of samples ($N = 14$) is 57.79 ± 7.64 mT (and the mean without sample XT-4.1 is 56.50 ± 6.16 mT). Samples used for the study come from sites CU-2, CU-3, CU-8, XT-4, and XT-7 (Fig. 1). The palaeointensities for samples from the university

campus are lower than those for the sites on the Ajusco slope. Samples studied in Nagata et al. (1965) come from a locality close to site CC-1, and those studied in Gonzalez-Huesca (1992) come from a site inside the campus. From the new data, it seems that lower values are obtained for the campus lavas. However, the two samples with lowest values were determined using the Shaw method (determinations using the Shaw method appear consistently lower than those obtained using the Thellier method; this was also noted by Gonzalez-Huesca (1992), who applied the two methods in samples from the same site). However, the data with higher values of Gonzalez-Huesca (1992) are for samples in the campus. At present, it seems difficult to determine with confidence any spatial pattern in the palaeointensity determinations. Nevertheless, what is interesting in the

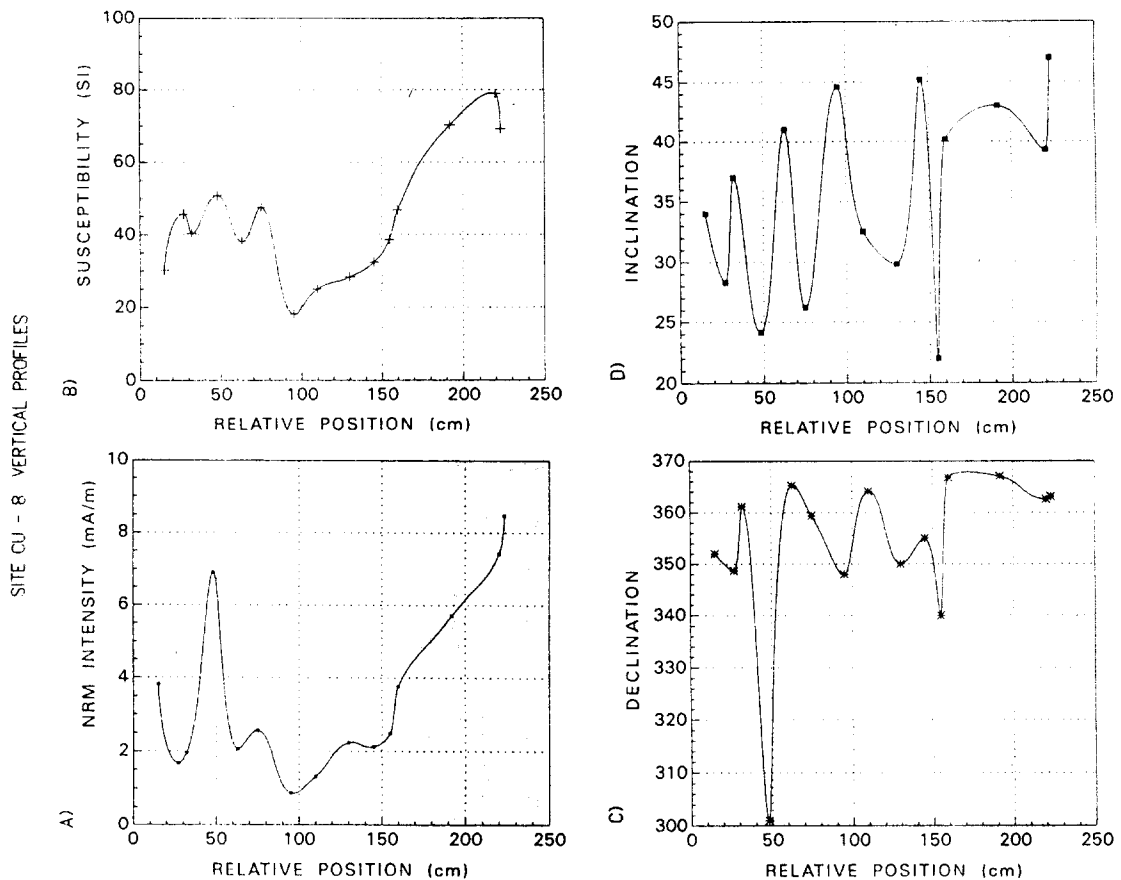


Fig. 9. Variation of palaeomagnetic properties across a vertical section. (a) NRM intensity, (b) low-field magnetic susceptibility, (c) declination and (d) inclination. Data for site CU-8.

palaeointensity data is the dispersion of values observed in the three studies (Table 3). The dispersion is not reduced by augmenting the number of determinations, and the overall mean for 20 palaeointensities (which is a high number of determinations for a single lava flow) shows a relatively high standard deviation (Table 3).

A mean palaeointensity estimate obtained by combining the Nagata et al. (1965) and the new data set shows a distribution approaching a normal gaussian distribution with a small standard deviation. The mean is $N = 13$, 56.50 ± 6.16 mT. Two samples analysed in Nagata et al. (1965) correspond to pottery (MP-1 and MP-2, Table 3) excavated in the

Cuicuilco site. The corresponding palaeointensity determinations are similar to those obtained for the volcanic samples, showing similar dispersion with a low and a high value (Table 3).

4. Discussion

The new data from different parts of the volcanic field (Fig. 1) show well defined characteristic directions with small within-site angular dispersions (Table 1). Particularly gratifying is the good coherence of directions over large horizontal distances, from close to the vent and farther away (over 12 km of horizontal distance). The overall mean direction ($B = 26$, $\text{Dec} = 359.8^\circ$, $\text{Inc} = 32.8^\circ$, $k = 167$, $\alpha_{95} = 2.2^\circ$) is characterized by small angular dispersion and inclination close to the dipolar value for the locality (see also mean direction calculated for all 28 sites; Table 1).

This overall mean direction can be considered as a reasonable result for a lava flow. Closer inspection, however, shows relatively large apparently consistent between-site differences, particularly in the mean inclinations. Discussion below concentrates on these between-site differences in directions and searches for possible explanations. First, we examine if the differences are statistically significant, and then we explore which directions, if any, may be considered as anomalous. By analysing the site mean directions and the apparent geographic dependence, an arbitrary cut-off inclination value of 30° was chosen to separate the data. The mean direction for sites with inclinations shallower than 30° is $\text{Dec} = 1.5^\circ$, $\text{Inc} = 26.7^\circ$ ($\alpha_{95} = 3.3^\circ$, $k = 338$, $B = 7$) and for the other sites is $\text{Dec} = 359.0^\circ$, $\text{Inc} = 35.1^\circ$ ($\alpha_{95} = 2.1^\circ$, $k = 247$, $B = 19$). These two mean directions have cones of 95% confidence that do not overlap and are statistically different (McFadden and Lowes, 1981). To further investigate the site mean directional distribution, directions have been referred to the rotated space as defined by Hoffman (1984). This procedure was developed to study transitional data and permits the investigation of the pattern of angular deviations from the dipolar direction. Site-mean directions in the rotated space are given in Fig. 13. In this case, angular deviations are much smaller than for transitional directions. The sites with inclinations around

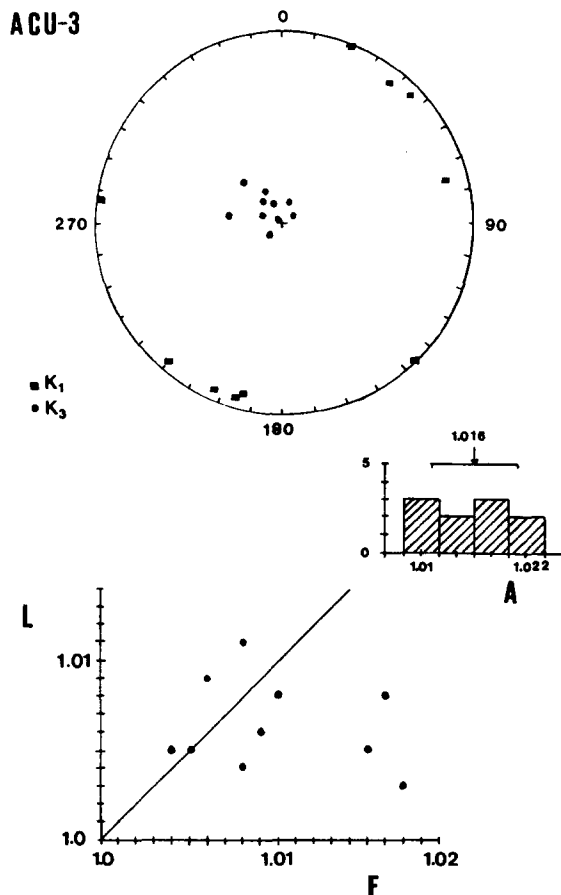


Fig. 10. Anisotropy of magnetic susceptibility (AMS) data for one of the sites ACU-3 in the university campus. (a) AMS principal axes k_1 and k_2 ; note that the k_3 axes are well grouped and close to the horizontal. (b) Lineation (k_1/k_2)/foliation (k_2/k_3) diagram. (c) Histogram for the degree of anisotropy (k_1/k_3).

the dipolar value for the area are clearly more numerous. There is unfortunately no independent direction for reference, and no way to conclusively estimate the corresponding geomagnetic field direction for the Xitle lava flow (and no way to conclusively identify any ‘anomalous’ directions). However, estimation of a direction for the locality calculated from the global virtual geomagnetic pole (VGP) compilation reported by Ohno and Hamano (1992) gives an inclination of 34.1° and a declination of 4.7° (reference pole is 85.5°N, 358.0°E, $N = 11$, $A_{95} = 4.4^\circ$, for 2000 years BP (radiocarbon time scale); Table 1 of Ohno and Hamano (1992). This calculated direction agrees better with the direction estimated for the volcanic field using the results close to the dipolar inclination value.

With the new data, the difference in the expanded data set between the shallow inclination and dipolar inclination sites decreased, but the two apparent

directional groups remain. The distinction between the ‘shallow’ and ‘dipolar’ inclination sites which was clear in the earlier data set is not so simple in the expanded data set. Nevertheless, there are some additional indications. Sites with the shallow inclinations correspond to localities farther from the Xitle vent, in the low altitude, gentle slope (flat) terrain. This apparent correlation with the terrain characteristics that influenced the lava emplacement suggests that the magnetizations might be influenced by the lava emplacement process. The overall vector mean (Table 1) has an inclination close to the dipolar value. Plotting the inclination anomaly (Fig. 14(a)) ($\Delta I = \text{observed inclination less the dipolar inclination}$) or the site-mean inclinations as a function of site altitude (or distance from vent) shows a peculiar distribution as mentioned above, with the occurrence of ‘anomalous’ sites preferentially located in the low area, within the university campus and farthest away

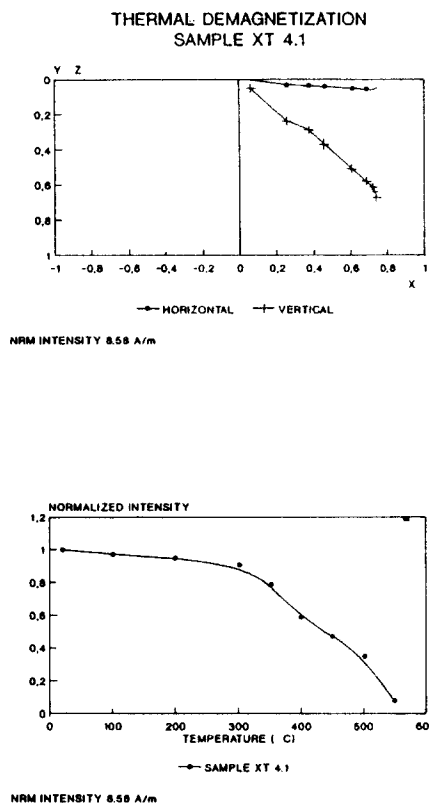
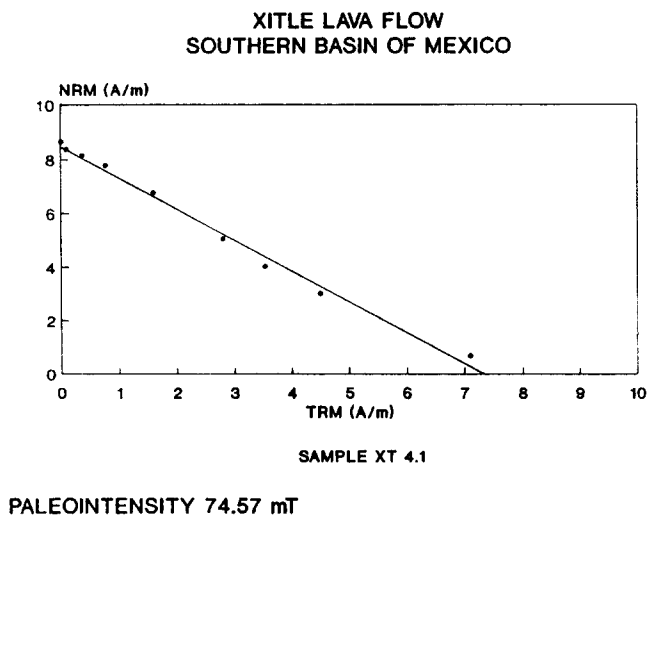
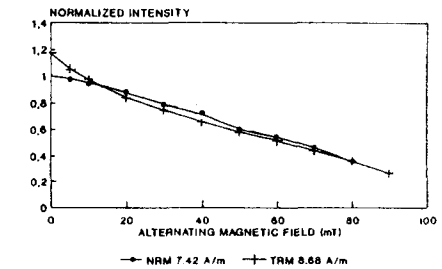
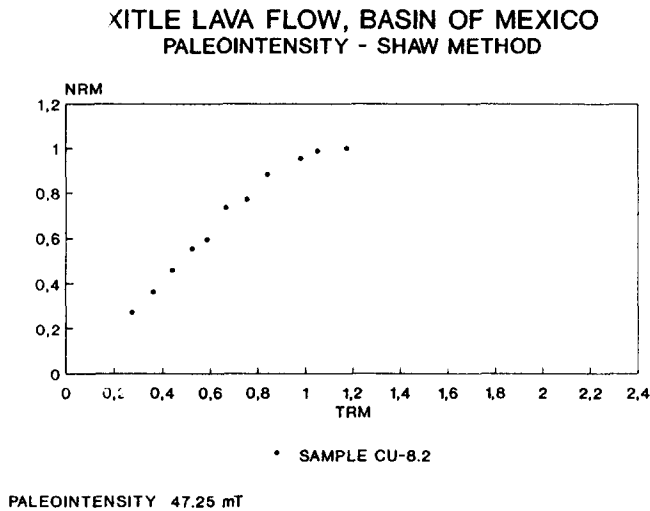


Fig. 11. Example of a palaeointensity determination using the Thellier method. Sample from site XT-4. See Table 3 for summary of the palaeointensity data.

from the Xitle vent (Fig. 15). Within-site dispersion (α_{95}) also displays a similar pattern (Fig. 14(b)). These observations stress the possibility that there are some effects associated with conditions and properties of the emplacement process and cooling history.

Results from one of the sites (CU-5) that presents a very shallow inclination (15°) show a relationship with a lava structure. Samples come from a flank of a pressure crest (in one of the walls of the fissure) and partial correction with 70% unfolding increases the inclination and brings it close to the dipolar value (and overall mean value). This indicates that the lava was cooling down when still subjected to movement and so, after the magnetization was fixed, it was rotated, resulting in a shallow inclination (with small dispersion and no secondary overprints). However, there are no comparable structures in the other sites and from the vesicle pattern (flattened vesicles aligned along horizontal planes in top part of flows) it appears the flows are essentially horizontal.

Another potential effect in the early results is the magnetic influence of outcrop in the orientation of samples. However, while this can contribute to the within-site dispersion estimates, it is not clear how it can give rise to preferentially shallow inclinations. For instance there is no statistically significant difference between the previous overall mean direction obtained using magnetic orientation, and the new one using both solar and magnetic compass orientation. Within-site dispersions are, however, lower using the solar compass orientation data. Measurements of the ground magnetic field anomalies were obtained using a total-field cesium Geometrics G-826 magnetometer at site CU-5 and in the university sculptoric centre close to site CU-8 (Fig. 1). Measurements display large amplitude variations with shortwave lengths, particularly inside the pressure crests, pits and fractures. Inside the pressure crest at site CU-5, the field was up to 5000 nT less than immediately outside the crest. That is, localized anomalies of some 10–15% of the total geomagnetic field appear



SAMPLE CU - 8.2 XITLE FLOW

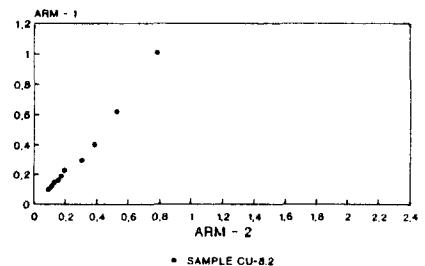


Fig. 12. Example of a palaeointensity determination using the Shaw anisothermic remanent magnetization method. Sample from site CU-8. See Table 3 for a summary of palaeointensity data.

common close to surficial features in the lava flow. Measurements with a three component fluxgate magnetometer not available for this study may be able to map directional variations over the lava flow and their influence in the magnetic orientation.

While magnetic properties vary from base to top of flows, there are no comparable systematic variation patterns in the NRM or characteristic direction. This factor may, however, contribute to the observed scatter, depending on where samples are collected. Sites in blocky lava fronts do not provide good data. One such site gave scattered directions, though it was clearly not a promising site from the start since blocks appeared to have been rotated.

Secular variation effects or a non-dipole field component are another candidate to produce system-

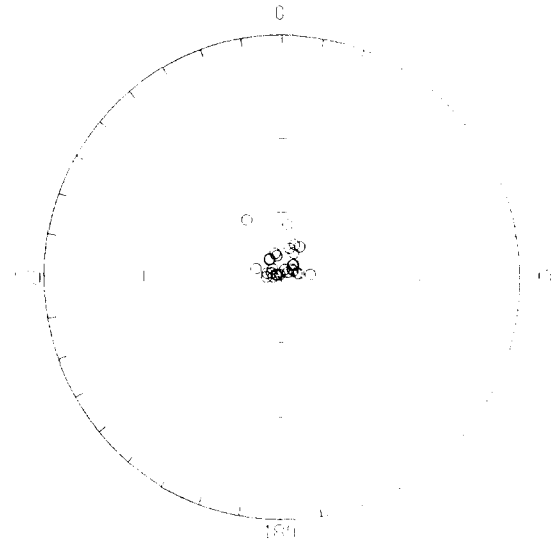


Fig. 13. Plot of site mean directions in the rotated space (algorithm for vector rotation after Hoffman, 1984). See text for discussion.

Table 3
Paleointensities for the Xitle-Pedregal de San Angel

Sample	Paleointensity (mT)	Method	Ref.
MP-1	65.34	Thellier	NKS-65
MP-5	54.15	Thellier	NKS-65
M-7	52.81	Thellier	NKS-65
M-8	47.44	Thellier	NKS-65
M-9	60.42	Thellier	NKS-65
M-10	51.02	Thellier	NKS-65
M-13	56.84	Thellier	NKS-65
M-14	60.86	Thellier	NKS-65
Mean $N = 8$	56.11 ± 5.89		
S-9B	76.64	Thellier	G-92
S-9C	54.23	Thellier	G-92
S-9E	59.33	Thellier	G-92
S-9H	79.40	Thellier	G-92
S-9I	70.03	Thellier	G-92
S-9K	119.80^a	Thellier	G-92
S-9Git	61.35	Shaw	G-92
S-9Sin	37.19	Shaw	G-92
Mean $N = 6$	66.83 ± 10.09		
CU-2.1	53.10	Shaw	This work
CU-8.2	47.25	Shaw	This work
CU-3.2	58.40	Thellier	This work
XT-7.2	66.09	Thellier	This work
XT-4.1	74.57	Thellier	This work
XT-7.1	60.80	Thellier	This work
Mean $N = 6$	60.04 ± 9.62		
Mean $N = 14$	57.79 ± 7.64	(NKS-65 and this work)	
Mean $N = 20$	60.50 ± 9.21	(all data)	

^a without S-9K.

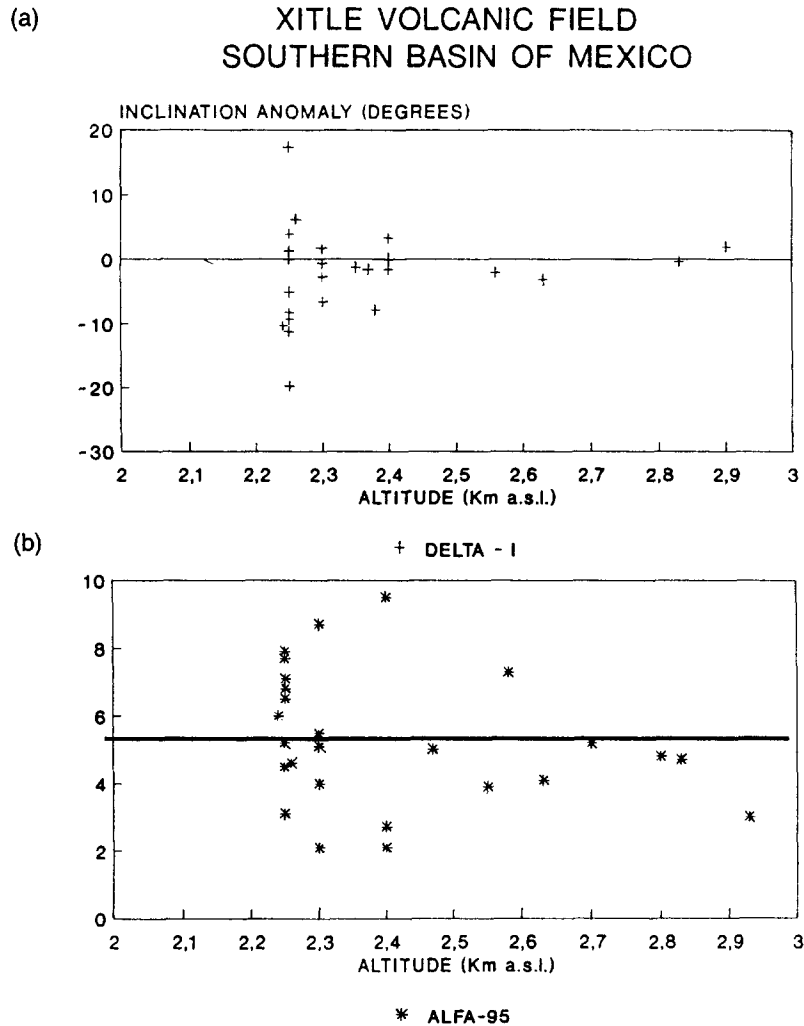
References: NKS-65, Nagata et al. (1965); G-92, Gonzalez-Huesca (1992).

atic angular differences. However, in the cases studied there seem to be no appreciable difference between flow units at single outcrops. Although the Xitle eruption was probably witnessed by the local inhabitants there are unfortunately no written accounts of the activity. Historic eruptions of similar volcanoes in the Mexican volcanic belt suggest short periods of activity, of the order of a decade or so (e.g. 1943–1953 Paricutin or the 1759–1774 Jorullo eruptions; Bullard, 1976). Further, palaeosecular variation (PSV) studies, using the angular dispersion of virtual geomagnetic poles, indicate a low PSV (comparable to that in the Hawaiian islands) for central Mexico during the recent part of Brunhes chron (i.e. past 60 to 100 000 years) (Böhnel et al., 1990; Urrutia-Fucugauchi, 1995). Small PSV may also characterize the historic period since 1923 AD, with observatory data (Urrutia-Fucugauchi and Campos-Enriquez, 1993).

Anomalous shallow inclinations (some 6° shallower than the observed geomagnetic field) have been reported earlier, for historic lava flows from Hawaii, 1950 eruption of Mauna Loa, and 1972 eruption of Kilauea (Castro and Brown, 1987; Tanguy, 1990). Several possible explanations were analysed, including sampling and measurement errors,

deformation and movements during flow and after cooling, secondary magnetizations, and shape anisotropy (high magnetic refraction effects). Deflection related to the shape anisotropy is generally small, of the order of a couple of degrees (Coe, 1979). Castro and Brown (1987) suggested that the effect may have been enhanced by the accumulation of lava flows. However, Tanguy (1990) points out that this

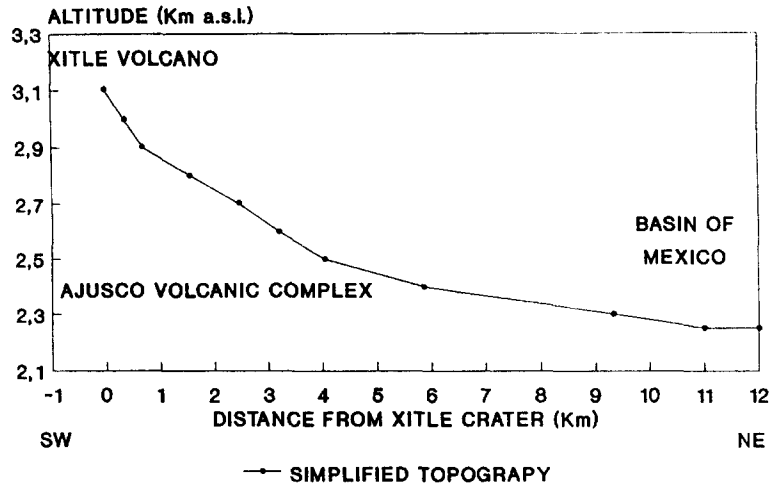
is not supported by the magnetic field measurements that showed steeper inclinations and that the volcanic pile is not substantially different from those of other volcanoes like Mount Etna and Piton de la Fournaise where inclination deflections are smaller than 2° (Tanguy, 1970). Tanguy (1990) noted a relationship between the inclination and the NRM intensity, where shallow inclinations corresponded to strong intensity



DIPOLAR INCLINATION 36 DEGREES

Fig. 14. (a) Inclination anomaly (dipolar inclination minus observed inclination) plotted as a function of altitude for the site. Note the occurrence of several sites with large ΔI in the lower (topographic) portion of the volcanic field. (b) Angular dispersion (α_{95}) for site directions plotted as a function of altitude for the sites.

XITLE VOLCANIC FIELD SCHEMATIC TOPOGRAPHIC PROFILE



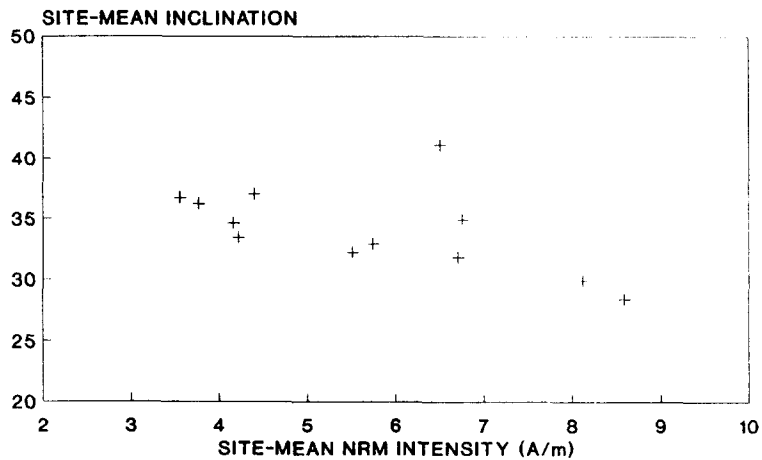
SOUTHERN BASIN OF MEXICO

Fig. 15. Changes with altitude and distance from vent. (a) Simplified topographic profile (oriented N–NE; see Fig. 1) from the Xitle volcano to the university campus, inside the basin. The Xitle volcano is located on the slope of the Ajusco volcano and the lava emplacement was controlled by the topographic relief.

values. He suggested that the demagnetizing effect could be unusually high in some sectors of the Mauna Loa lava flows. He also suggested that even

in sectors with average intensities, directions could be affected by the local field distortion due to strongly magnetized neighbouring parts. The results for the

PEDREGAL DE SAN ANGEL LAVA FIELD



+ Series 2

Fig. 16. Site mean inclinations plotted as a function of its mean NRM intensities for the new sites studied in the Xitle–Pedregal de San Angel.

1972 Kilauea flows show variations along the length of the flows and within vertical sections (Castro and Brown, 1987).

Tanguy (1990) found very strong magnetizations, with values higher than 10 A m^{-1} and up to 35 A m^{-1} in his studies, but the NRM intensities from the Xitle-Pedregal de San Angel flows are not that high, being between about 2.5 and 13 A m^{-1} . The expected deflection due to the shape of the lava flow will be too small to account for the angular difference observed (Coe, 1979; Tanguy, 1990) and some characteristic specific to certain sectors of the Xitle-Pedregal de San Angel flow must be involved. There is, however, a relationship between site mean inclinations and site mean NRM intensities (Fig. 16), with higher intensities corresponding to the shallow inclinations.

Six palaeointensity determinations using the Thellier and the Shaw methods give a mean of $60.04 \pm 9.62 \text{ mT}$. Deletion of one sample gives a mean of $57.13 \pm 7.23 \text{ mT}$, which is close to the mean calculated for eight samples reported earlier by Nagata et al. (1965) of $56.11 \pm 5.89 \text{ mT}$. The angular standard deviation is relatively high. The combined mean of the two data sets is $56.50 \pm 6.16 \text{ mT}$ ($N = 13$), which also presents a high standard deviation that seems to be a characteristic of the flow (or the methods). Results obtained in this study give three lower palaeointensity values for sites in the campus compared with those three closer to the Xitle vent on the Ajusco slope. However, two of the low values have been obtained by the Shaw method, and it may be a methodological factor involved. Studies directed to compare the two methods have generally reported good agreement. For instance, Aitken et al. (1988) summarized results for 31 samples studied by the two methods and reported Shaw/Thellier ratios varying between 0.75 and 1.25, with a mean ratio of 1.01 and a small standard deviation of 0.10. Additional data reported in Gonzalez-Huesca (1992) give higher values, with a mean of $66.83 \pm 10.09 \text{ mT}$ ($N = 6$). We note that in that study, the two results obtained with the Shaw method are also lower than those obtained with the Thellier method. Comparison of data obtained solely with the Thellier method shows a large standard deviation. There seems to be methodological factors involved, as well as factors related to the magnetic record of the lava flow (see

e.g. Walton, 1988; Aitken et al., 1988). The number of palaeointensity determinations is relatively high for a single monogenetic volcano and the overall mean has a relatively large standard deviation ($N = 20$, $60.50 \pm 9.21 \text{ mT}$; Table 3).

Results show that careful analysis needs to be exercised when interpreting apparently anomalous data from young apparently 'quite suitable' volcanic lava flows. There are, for example, two directional groups for the Xitle-Pedregal de San Angel volcanic field. The group with more sites ($B = 19$) and which are distributed along the entire field shows an inclination close to the dipolar value and may be considered representative for the Xitle-Pedregal de San Angel. The other group with shallow inclinations is less numerous ($B = 7$) and seems to have a restricted occurrence in a particular location of the volcanic field.

Acknowledgements

Critical comments provided by the journal referees have been useful in preparing the manuscript and are greatly appreciated. Thanks are due to Beatriz Ortega for assistance with this study and to Francisco Torres for lending us the Geometrics G-826 cesium magnetometer. Partial economic support from UNAM DGAPA projects IN-103589 and IN-103292 and the Ricardo J. Zevada Scientific Foundation is gratefully acknowledged.

References

- Aitken, M., Allsop, A.L., Bussell, G.D. and Winter, M.B., 1988. Determination of the intensity of the Earth's magnetic field during archaeological times: Reliability of the Thellier technique. *Rev. Geophys.*, 26: 3–12.
- Arnold, J.T. and Libby, W.F., 1951. Radiocarbon dates. *Science*, 113: 111–120.
- Badilla-Cruz, R.R., 1977. Estudio petrológico de la lava de la parte noreste del Pedregal de San Angel. *D.F. Bol. Soc. Geol. Mex.*, 38: 40–57.
- Böhnel, H., Urrutia-Fucugauchi, J. and Herrero-Bervera, E., 1990. Palaeomagnetic data from central Mexico and their use for paleosecular variation studies. *Phys. Earth Planet. Inter.*, 64: 224–236.
- Bullard, F.M., 1976. *Volcanoes of the Earth*. University of Queensland Press, Saint Lucia.

- Castro, J. and Brown, L., 1987. Shallow palaeomagnetic directions from historic lava flows, Hawaii. *Geophys. Res. Lett.*, 14: 1203–1206.
- Centeno-Garcia, E., Urrutia-Fucugauchi, J. and Herrero-Bervera, E., 1986. Diferenciación y caracterización de flujos de la vapor medio de sus propiedades magnéticas-Pedregal de San Angel, Mexico. *Mem. Reunion Anual, Union Geofis. Mex.*, 1: 464–471.
- Coe, R.S., 1979. The effect of shape anisotropy on TRM direction. *Geophys. J.R. Astron. Soc.*, 56: 369–383.
- Coe, R.S. and Grommé, C.S., 1973. A comparison of three methods of determining geomagnetic paleointensities. *J. Geomag. Geoelectr.*, 25: 415–435.
- Cordova, C., Martin, A.L. and Lopez, J., 1994. Palaeolandforms and volcanic impact on the environment of prehistoric Cuicuilco, southern Basin of Mexico. *J. Archaeol. Sci.*, 21: 585–596.
- Crane, H.R. and Griffin, J.B., 1958. University of Michigan radiocarbon dates III. *Science*, 128: 1117–1123.
- Deevey, E.S., Gralensky, L.J. and Hoffren, V., 1959. Yale natural radiocarbon measurements IV. *Radiocarbon*, 1: 144–172.
- Fergusson, G.J. and Libby, W.F., 1963. UCLA radiocarbon dates II. *Radiocarbon*, 5: 1–22.
- Fergusson, G.J. and Libby, W.F., 1964. UCAL radiocarbon dates III. *Radiocarbon*, 6: 318–339.
- Fisher, R.A., 1953. Dispersion on a sphere. *Proc. R. Soc. London A*, 217: 295–305.
- Gonzalez-Huesca, I.S., 1992. La variación secular en México central durante los últimos 30,000 años por medio del estudio magnético de lavas. Doctoral Thesis, National University of Mexico, Mexico City.
- Gunn, B.M. and Mooser, F., 1970. Geochemistry of the volcanics of central Mexico. *Bull. Volcanol.*, 34: 577–616.
- Haggerty, S.E., 1976. Oxidation of opaque mineral oxides in basalts. In: D. Rumble III (Editor), *Oxide Minerals*. *Miner. Soc. Am., Short Course Notes*.
- Heizer, R. and Bennyhoff, J., 1958. Archaeological investigations of Cuicuilco, Valley of Mexico, 1956. *Science*, 127: 232–233.
- Heizer, R. and Bennyhoff, J., 1972. Archaeological excavations at Cuicuilco, Mexico, 1957. *Natl. Geogr. Rep.*, 1955–1960: 93–104.
- Herrero-Bervera, E. and Pal, S., 1978. Palaeomagnetic study of Sierra de Chichinautzin, Mexico. *Geof. Int.*, 17: 167–180.
- Hoffman, K.A., 1984. A method for the display and analysis of transitional palaeomagnetic data. *J. Geophys. Res.*, 89: 6285–6292.
- Irving, E., 1964. *Palaeomagnetism and Its Application to Geological and Geophysical Problems*. Wiley, 399 pp.
- Libby, W.F., 1955. *Radiocarbon Dating*. 2nd edn., Chicago University Press, Chicago, USA.
- Lowrie, W. and Fuller, M.D., 1971. On the alternating field demagnetization characteristics of multidomain thermoremanent magnetization in magnetite. *J. Geophys. Res.*, 76: 6339–6349.
- McFadden, P.L. and Lowes, F.J., 1981. The discrimination of mean directions drawn from Fisher distributions. *Geophys. J.R. Astron. Soc.*, 67: 19–33.
- Mooser, F., Nairn, A.E.M. and Negendank, J.F.W., 1974. Palaeomagnetic investigation of the Tertiary and Quaternary igneous rocks: VIII A palaeomagnetic and petrologic study of volcanics of the Valley of Mexico. *Geol. Rundsch.*, 63: 451–483.
- Nagata, T., Kobayashi, K. and Schwarz, E.J., 1965. Archeomagnetic intensity studies of South and Central America. *J. Geomag. Geoelectr.*, 17: 399–405.
- Ohno, M. and Hamano, Y., 1992. Geomagnetic poles over the past 10,000 years. *Geophys. Res. Lett.*, 19: 1715–1718.
- Ordoñez, E., 1890. El Pedregal de San Angel. Apuntes para la petrografía del Valle de México. *Mem. Soc. Cient. Antonio Alzate*, 4: 15.
- Ortega, B., Urrutia-Fucugauchi, J. and Nieto, J., 1993. Geología y edades de C-14 del derrame del Pedregal de San Angel. Technical Rep. Inst. Geof. UNAM, Mexico City.
- Pal, S. and Urrutia-Fucugauchi, J., 1977. Palaeomagnetism, geochronology and geochemistry of some igneous rocks from Mexico and their tectonic implications. In: IV Int. Gondwana Symp., Calcutta, India. Vol. 1. Hindustan Publishing Corp., Delhi, pp. 814–831.
- Perez, J., Pal, S., Terrell, D.J., Urrutia-Fucugauchi, J. and Lopez-Martinez, M., 1979. Preliminary report on the analysis of some in-house geochemical reference samples from Mexico. *Geofis. Int.*, 18: 197–209.
- Shaw, J., 1974. A new method of determining the magnitude of the palaeomagnetic field. Application to five historic lavas and five archaeological samples. *Geophys. J.R. Astron. Soc.*, 39: 133–141.
- Schmitter, E., 1953. Investigación petrológica en las lavas del Pedregal de San Angel. *Mem. Congr. Cien. Mex.*, 3: 218–237.
- Stuiver, M. and Becker, B., 1993. High-precision decadal calibration of the radiocarbon timescale, AD 1950–6000 BP. *Radiocarbon*, 35: 35–65.
- Stuiver, M. and Pearson, G.W., 1993. High-precision calibration of the radiocarbon time scale, AD 1950 to 500 BC and 2500–6000 BC. *Radiocarbon*, 35: 1–23.
- Tanguy, J.C., 1970. An archaeomagnetic study of Mount Etna: The magnetic direction recorded in lava flows subsequent to the twelfth century. *Archaeometry*, 12: 115–128.
- Tanguy, J.C., 1990. Abnormal shallow palaeomagnetic inclinations from the 1950 and 1972 lava flows, Hawaii. *Geophys. J. Int.*, 103: 281–283.
- Thellier, E. and Thellier, O., 1959. Sur l'intensité du champ magnétique terrestre dans le passé historique et géologique. *Ann. Geophys.*, 15: 285–376.
- Urrutia-Fucugauchi, J., 1995. Constraints on Brunhes low-latitude paleosecular variation-Iztaccihuatl stratovolcano, Basin of Mexico. *Geof. Int.*, 34: 253–262.
- Urrutia-Fucugauchi, J. and Campos-Enriquez, J.O., 1993. Geomagnetic secular variation in central Mexico since 1923 AD and comparison with 1945–1990 IGRF models. *J. Geomag. Geoelectr.*, 45: 243–249.
- Urrutia-Fucugauchi, J. and Martin del Pozzo, A.L., 1993. Implicaciones de los datos paleomagnéticos sobre la edad de la Sierra de Chichinautzin, Cuenca de México. *Geof. Int.*, 32: 523–533.
- Urrutia-Fucugauchi, J. and Valencio, D.A., 1976. Estudio paleomagnético del basalto del Pedregal de San Angel, Valle de

- Mexico. Report Instituto de Geofísica, National University of Mexico (UNAM), Mexico City, 26 pp.
- Waltz, P. and Wittich, E., 1911. Tubos de explosión en el Pedregal de San Angel. *Bol. Soc. Geol. Mex.*, 7: 165–186.
- Walton, D., 1988. The lack of reproducibility in experimentally determined intensities of the Earth's magnetic field. *Rev. Geophys.*, 26: 15–22.
- White, S.E., Reyes, M., Ortega, J. and Valastro, S., 1990. El Ajusco: Geomorfología volcánica y acontecimientos glaciales durante el Pleistoceno Superior y comparación con las series glaciales mexicanas y las Montañas Rocallosas. *Colec. Cientif.*, INAH, Mexico City, 212: 1–77.